# Reusable Hollow Polymer Microreactors Incorporated with Anisotropic Nanoparticles for Catalysis Application

Varsha Sharma[†,‡] and Anandhakumar Sundaramurthy*[,†,§]

†SRM Research Institute, ‡Department of Biomedical Engineering, and §Department of Physics and Nanotechnology, SRM Institute of Science and Technology, Kattankulathur, Kancheepuram, Tamil Nadu 603203, India

ABSTRACT: We report a methodology to encapsulate gold nanorods (AuNRs) and gold bipyramids (AuBPs) into polyelectrolyte capsules for catalytic application. Microreactors (capsules with encapsulated NRs or BPs) were fabricated by sequential deposition of poly(allylamine hydrochloride) and dextran sulfate on modified sacrificial template, followed by core dissolution. AuNRs and AuBPs of size 25−30 nm were successfully encapsulated in the fabricated polyelectrolyte capsules and were stable and distributed uniformly in the interior. Fabricated microreactors were investigated as catalysts for the reduction of p-nitrophenol to p-aminophenol in the presence of sodium borohydride in aqueous phase. Reaction parameters such as order, conversion, and rate constants were estimated for microreactors and compared to free anisotropic nanoparticles in suspension. The reaction rate was higher for NRs in both free and capsule forms compared to BPs. Microreactors demonstrated excellent catalytic activity even after three times of use. Such capsules have high potential for use as microreactors in applications such as catalysis, drug delivery, imaging, and cancer chemo-photothermal therapy.
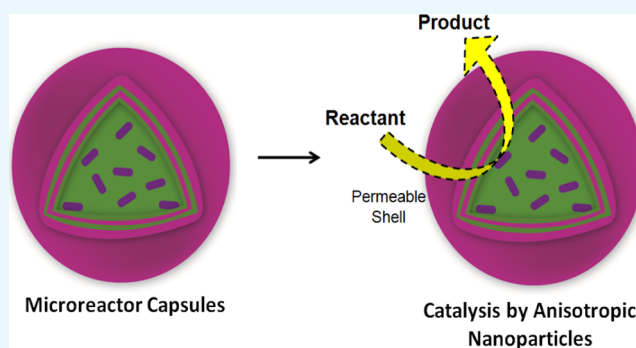
1. INTRODUCTION

In the past two decades, polymeric hollow capsules have shown great promise in the fields of catalysis, sensing, and drug delivery because of their ability to provide stable and well-dispersed colloidal microcarrier system. The unique features such as high encapsulation efficiency for biomolecules, selective permeability for the reactants, confined space for the interaction of reactants, easier separation of formed products, and possibility for surface modification make them a potential candidate for various applications.[1−3] Several strategies are being explored to fabricate polymeric capsules with novel architecture that can provide unique option to manipulate the capsule permeability and space to accommodate molecules in the inner cavity. Smart nanofactories,[4] polymersomes, dendrimers, micelles, stimuli-responsive nanocarriers,[5] artificial organelles,[6] artificial cells,[7] and other systems have successfully been reported for the fabrication of nano-microreactors for different biological applications.[8] Among the different methods reported for hollow capsule fabrication, the layer-by-layer (LbL) assembly owes its popularity to the fact that it provides access to near-perfect, ultrathin polymeric shell on the one hand while allowing precise tailoring of shell properties such as permeability, thickness, and composition on the other hand.[9−11] Interestingly, LbL-assembled capsules provide option to tune permeability based on our requirements. For instance, the shell permeability of the capsules can be reversibly tuned from open to closed states by varying environmental parameters such as pH, temperature, polarity, and ionic strength.[12−15] When burst release is needed, capsules can also be ruptured irreversibly by exposing to external triggers such as laser light, ultrasound, and magnetic field.[16−19] Successful encapsulation of various macromolecules (e.g., enzymes, proteins, genes, amino acids, and other bioactive materials), pharmaceutical drugs, and nanoparticles (NPs) into polyelectrolyte capsules has been reported by using them as micro- and nanocontainers.[1,20]

NPs, especially gold NPs, are preferred for several chemical oxidation and reduction reactions compared to their counterpart bulk gold, owing to their high surface-to-volume ratios and unique physical and chemical properties.[21] They have been widely used as catalysts for several oxidation and hydrogenation reactions, carbon−carbon coupling reactions such as homocoupling of halides and organoboronates, and A3 coupling reactions of amines, phenylacetylenes, and aldehydes.[22] With the emergence of novel methodologies to synthesize gold anisotropic nanoparticles (ANPs) (gold nanorods (AuNRs), gold bipyramids (AuBPs), gold nanoprisms, etc.), several reports have demonstrated their excellent catalytic properties. For instance, higher rate constant and lower conversion time were observed for the conversion of p-nitrophenol (PNP) to p-aminophenol (PAP) using NaBH4 catalyzed by AuNRs with an aspect ratio of 3.3 (length, 40 nm; diameter, 12 nm) compared to spherical nanospheres of size 20 nm.[23] Interestingly, the conversion is largely dependent on

the size of spherical ANPs. When larger spherical NPs (40 nm) and smaller ANPs (aspect ratio, 2.8) were used for same catalytic reaction, complete conversion was achieved within 64 min for spherical NPs.[24] However, it took 118 min for AuNRs and 87 min for gold nanoprisms. As nanoprisms have more well-defined edges and corners compared to AuNRs, they provided more catalytic sites for the conversion of PNP to PAP and resulted in high rate of reaction. It should also be noted that there are inconsistencies in the results found in the literature, which is probably due to different masses of catalysts used for experiments. Furthermore, gold nanoantennas with shorter protrusions displayed higher rate constant for PNP to PAP conversion compared to longer protrusions owing to the more efficient PNP adsorption on its surfaces.[25] Another important factor that alters the reaction rate is the effect of spatial orientation and packing pattern of the particles.[26] In all cases, the number of particles was kept constant by applying different ways such as maintaining the same amount of gold salts for NP synthesis or the weight of the particles. However, the methodologies mentioned above assume that the conversion is uniform, which is not true. Hence, a detailed investigation is necessary to estimate the rate constants by including the PNP concentration and the number of ANPs used for the conversion. Alternatively, the amount of catalyst NPs required to convert 1 unit mole of PNP along with rate constants might provide better information on the effectiveness of catalyst NPs. Furthermore, issues such as aggregation of NPs, separation of catalyst NPs after reaction, and non-reusability limit their potential and pose an open question in applicability of ANPs in catalysis.

Novel methods are being explored to encapsulate ANPs into the hollow capsules as it enhances their regulation and reusability as catalysts. Further, separation of catalyst NPs is easier and cost-effective when they are used in encapsulated form (microreactors). Hollow capsules with encapsulated NRs are demonstrated for cancer therapy, biological imaging, and theranostics.[27,28] Some of these strategies follow the growth of NPs on the polymer shell, while others follow the growth of ANPs inside the capsule via either *in situ* growth of NRs in the core before polymer deposition or modification of template using preformed NRs. However, only few reports have successfully presented the latter, and the yield of NRs observed was also very minimal.[29] Furthermore, only NRs were reported by using the above-mentioned methodologies. In the perspective of catalysis, the lower amount of encapsulation of NRs (yield) might significantly affect the conversion of reactants into products. When microcapsules of poly-(allylamine hydrochloride) (PAH) and poly(styrenesulfonate) (PSS) containing spherical silver NPs in their shell were used for the reduction of PNP to PAP, 100% conversion was achieved after 12 h and the reaction rate was much lower as direct surface of the particles was not exposed for reaction.[30] Interestingly, the progress of the reaction can be stopped by increasing the number of bilayers to eight as it prevents the contact of catalysts and reactants. Similarly, a comparative study of NPs in encapsulated and free forms demonstrated lower catalytic activity for the former during the reduction of hexacyanoferrate(III) by borohydride ions.[31] The advantage of encapsulated system is that it provides the space and ability for further modification with other molecules or NPs (e.g., magnetic NPs) that could enable easy separation of catalysts at the end of reaction using magnetic separation. Microcages made of silver NPs showed excellent catalytic activity for the

epoxidation of higher olefins even after four successive uses.[32] Hairy hybrid nanorattle polymer shell containing platinum NPs was used as nanocatalyst for pseudo-first-order kinetic reduction of PNP.[33] The rate of reduction increased as a function of temperature. The catalyst recovery was easy after completion of the reaction along with excellent reusability even after three times of use with no loss in efficiency. Polymer capsules of poly(ionic liquid) and poly(2-(dimethylamino)-ethyl methacrylate) (PDMAEMA) containing AuNPs were also shown to catalyze the conversion of PNP to PAP. Notably, the rate of reaction increased continuously until the reaction temperature reached lower critical solution temperature of PDMAEMA at 50 °C.[34] The catalyst showed excellent reusability with slightly decreased reaction conversion after running for five cycles.

It is important to note that microcapsules encapsulated with spherical NPs are widely explored, but there are no reports on ANPs encapsulated in micro- or nanocapsules for catalysis applications. To the best of our knowledge, this is the first report on encapsulation of ANPs into hollow polyelectrolyte capsules for catalysis application. In this work, we have fabricated PAH/dextran sulfate (DS) microcapsules loaded with AuNRs/AuBPs in the interior of the hollow structure via modified core template method. The sacrificial template was prepared by adding preformed AuNRs or AuBPs during the synthesis of $CaCO_3$ microparticles. The present method shows excellent distribution and encapsulation of NRs/BPs in the interior of the capsules. Fabricated microreactors and free ANPs were investigated using UVvisible (UV−vis) spectroscopy and transmission electron microscopy (TEM). These microcapsules were investigated for catalytic conversion of PNP to PAP in aqueous phase with $NaBH_4$. Reaction parameters such as order, rate constants, and conversion time were estimated for microreactors and compared with ANPs in suspension.

2. RESULTS AND DISCUSSION

2.1. Fabrication of ANPs and Microreactor Capsules. For the fabrication of microreactors, NRs or BPs of 25−30 nm in length were prepared by seed-mediated approach and incorporated into sacrificial $CaCO_3$ template prior to LbL assembly process. By using this modified $CaCO_3$ particles as sacrificial template, hollow capsules (microreactors) were prepared by sequential deposition of PAH and DS, followed by core dissolution with 0.2 M ethylenediaminetetraacetic acid (EDTA) solution. NRs and BPs were chosen for catalytic experiments as they can be synthesized via seed-mediated method using cetyl trimethylammonium bromide (CTAB) as a stabilizing agent. Furthermore, previous reports demonstrated that the presence of CTAB on the surface of NPs did not affect their catalytic activity. For instance, 100% catalytic activity was achieved in 64 and 120 min for CTAB-stabilized positively charged gold nanospheres of diameter 45 ± 5 nm and NRs of aspect ratio 2.8 ± 0.2, respectively.[24]

A two-step synthesis method was adopted to synthesize NRs and BPs. Initially, seed crystals of size ∼4 nm were prepared by reducing $HAuCl_4$ using strong reducing agent $NaBH_4$ in the presence of CTAB or trisodium citrate. The seed crystals were then allowed to grow into NRs or BPs by controlling their growth via modulating the concentrations of $AgNO_3$, shape-directing agent (CTAB), and weak reducing agent ascorbic acid (AA). The formation of NRs and BPs was investigated using UV−vis spectroscopy and TEM. Notably, UV−vis
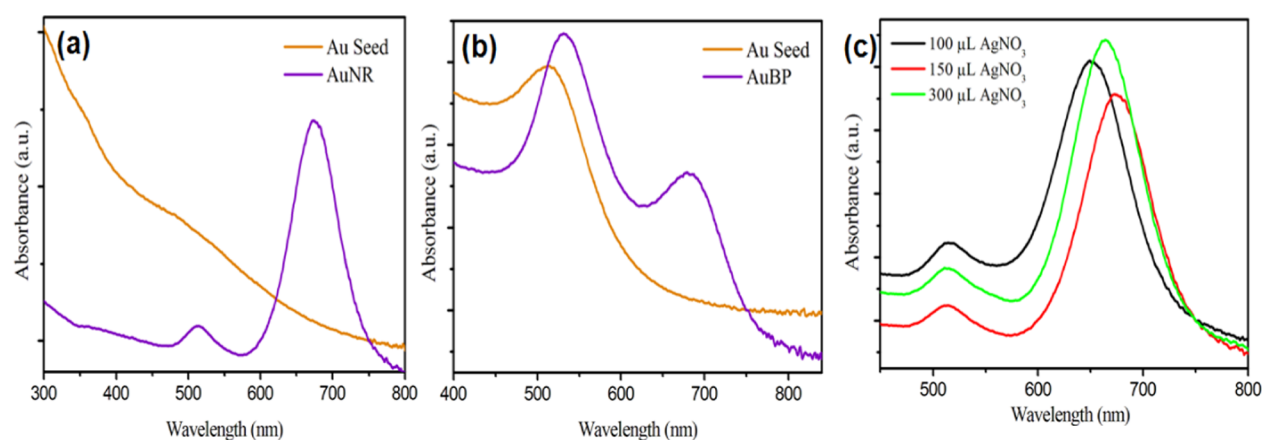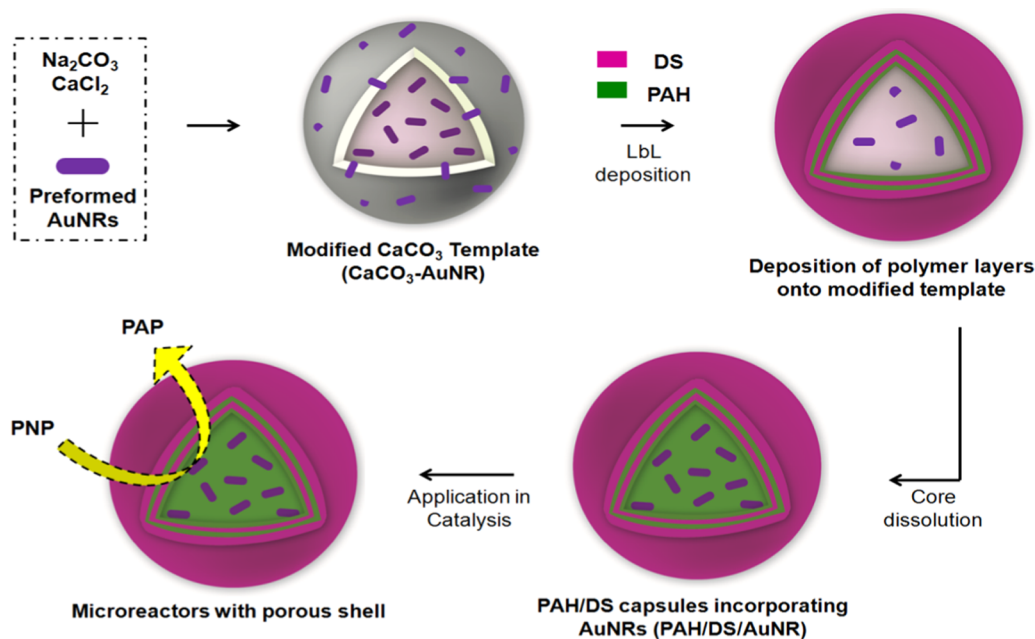
Figure 1. UV−vis spectra of synthesized (a) AuNRs and (b) AuBPs, and (c) different aspect ratios of AuNRs.
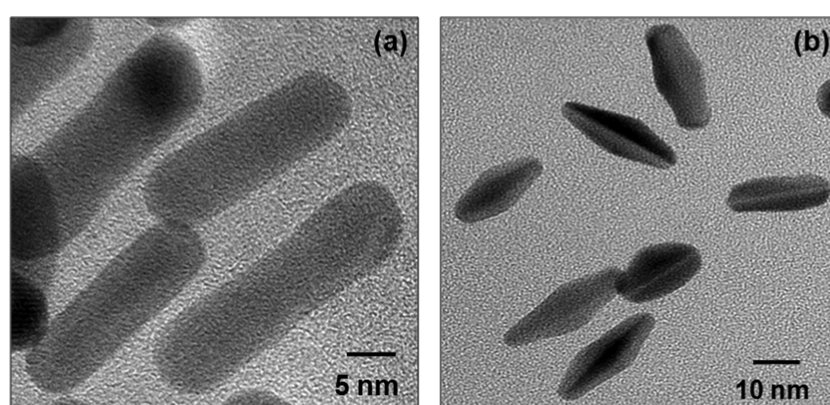
Figure 2. TEM investigations showing the morphology of synthesized (a) AuNRs and (b) AuBPs.

Scheme 1. Schematic Illustration of the Fabrication of Microreactors by LbL Methodology[a]

[a]Modified templates with preformed ANPs (AuNRs or AuBPs) were used as sacrificial templates for the fabrication of hollow capsules.

spectrum of seed crystals showed a characteristic absorption band for gold NPs at 475 nm (Figure 1). AuNR spectrum showed two new peaks at 513 and 673 nm, which correspond to transverse and longitudinal bands of NRs. Aspect ratio of AuNRs was easily varied by changing the $AgNO_3$ concentration (100, 150, and 300 μL) in the growth solution, as
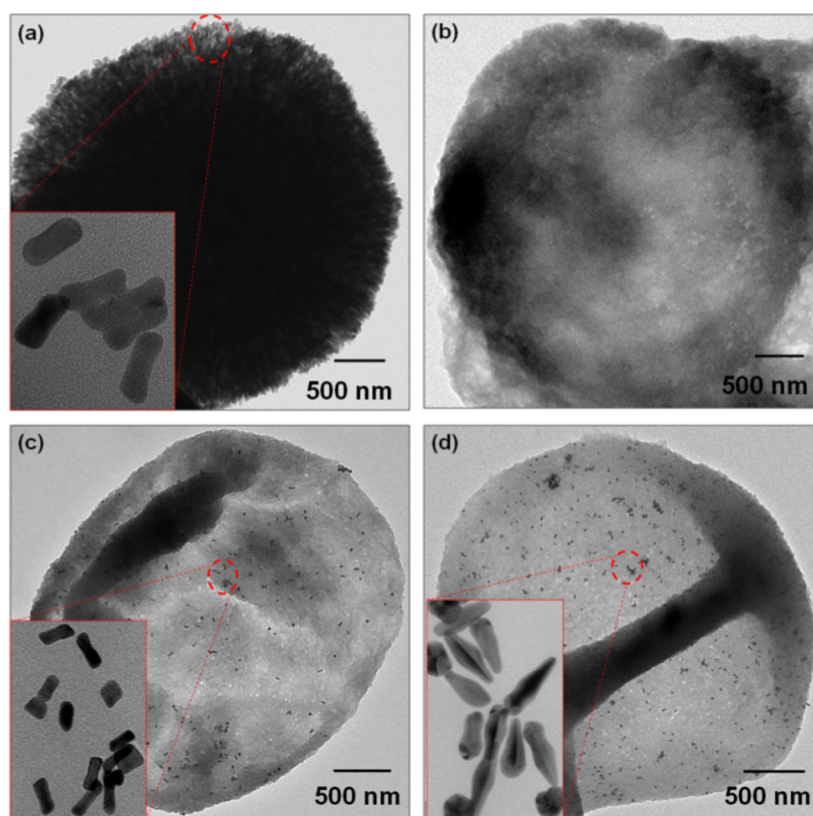
Figure 3. TEM investigations of the morphology of the synthesized CaCO$_3$–ANPs microparticles and microreactors. (a) CaCO$_3$–AuNR-modified template, (b) control (PAH/DS)$_2$ capsules, (c) PAH/DS/AuNR microreactor capsules, and (d) PAH/DS/AuBP microreactor capsules.

shown in Figure 1c. The red shift in the longitudinal band depicts the increase in aspect ratio of AuNRs from 2 to 4.7.[35] Similarly, seeding growth process was used for faceted BP– NPs formation, wherein seed crystals showed a characteristic absorption band at 515 nm. The growth solution "A" produced highly faceted gold NPs, which were then grown into bipyramidal structures in the growth solution "B". The bands formed at 530 and 680 nm were corresponding to transverse and longitudinal bands of BPs. TEM investigations showed that NRs as well as BPs were well dispersed and stable. The diameter and length of NRs were about 8 ± 1 and 30 ± 2 nm, respectively, i.e., aspect ratio (L/D) of about 4 ± 0.3 (Figure 2). Similarly, the average length of the BPs was about 25 nm; however, it depends on the number of intermediate steps used for the growth process.[36] Sequential addition of AA, CTAB, and AgNO$_3$ during the growth resulted in multifaceted growth into bipyramid structures.

The microreactor capsules with NRs and BPs were fabricated using LbL deposition of alternate layers of PAH and DS over modified CaCO$_3$ templates as illustrated in Scheme 1. Mixing of preformed AuNRs or AuBPs with Na$_2$CO$_3$ during template preparation resulted in CaCO$_3$ microparticles with incorporated NRs (CaCO$_3$–AuNR) or BPs (CaCO$_3$–AuBP), as shown in Figure 3a. The template particles obtained were well dispersed and stable with size of 3.5 ± 0.25 μm. Notably, NRs of about 30 nm were visible on the surface of modified CaCO$_3$–AuNR templates (inset in Figure 3a). This negatively charged modified core was then coated sequentially by two bilayers of PAH (positively charged polymer) and DS (negatively charged polymer) (PAH/DS)$_2$, with PAH being the first layer. Hollow microreactor capsules

incorporated with ANPs were obtained by dissolving the modified sacrificial template with 0.2 M EDTA (Figure 3). The obtained capsules appeared with folds and creases that were typical for hollow capsules of thin polymeric shell. Notably, the AuNRs or AuBPs were distributed uniformly within the shell, confirming their successful encapsulation. The yield of ANPs was apparently high, and there was no sign of aggregation. The shell thickness was estimated from TEM investigations, which was about 200 nm.

2.2. Catalytic Conversion of PNP to PAP. Catalyst NPs in free and capsule forms were investigated for catalyzing the reduction of nitro compound PNP to PAP in aqueous phase using NaBH$_4$ to evaluate their potential in catalysis application. As reduction of nitrophenol is a common starting or intermediate step in organic reactions, we have adopted this reaction to evaluate the potential of synthesized catalysts. The movement of NaBH$_4$ to catalyst surface results in hydride (Au–H species) formation on the surface, which is not only responsible for attracting PNP to surface but also reduces it to PAP.[37] Previous reports demonstrated that the presence of positively charged CTAB on the NPs surface did not alter the rate of reaction. Although the reason was not clear, it was stated that a small amount of CTAB adsorbed on NPs surface did not affect the catalytic activity of ANPs or spherical NPs.[24] Interestingly, the rate of reaction is influenced by CTAB when the reaction is performed in CTAB solution. It was possible that positively charged CTAB in the solution might have reduced the transport of hydride ions to catalyst surface and hence played an important role in reducing the rate of reaction. Four types of catalyst samples, namely, free AuBPs, free AuNRs, PAH/DS/AuBP microcapsules, and PAH/DS/AuNR

Table 1. Details of Catalysts Used for Reduction Reaction

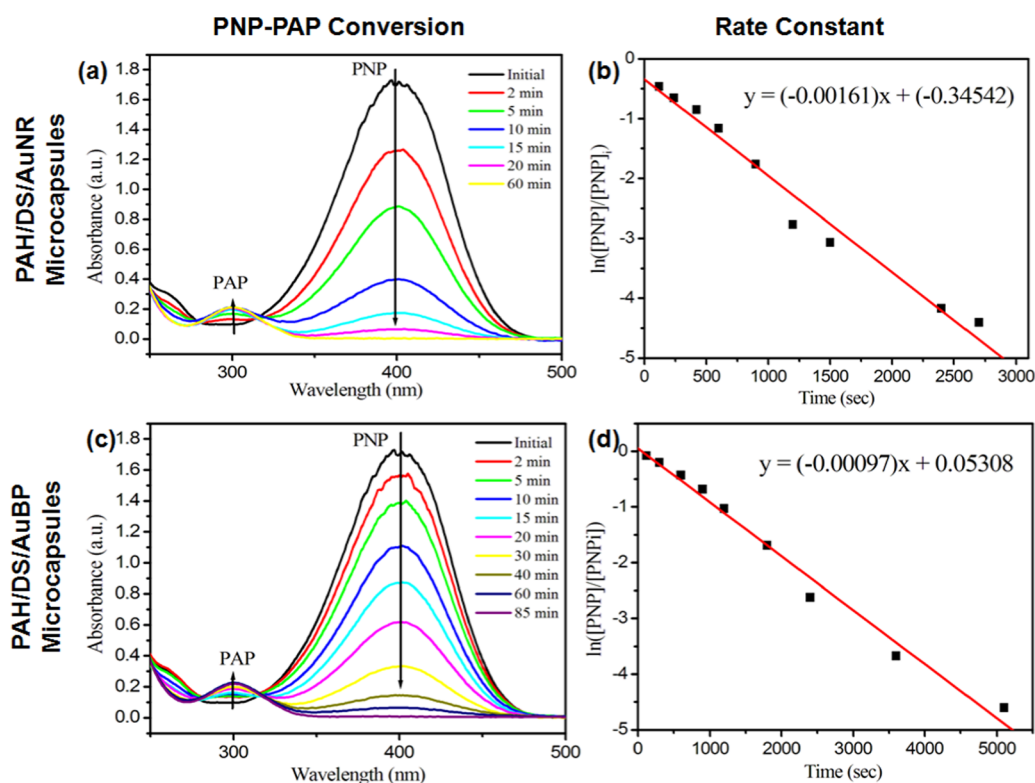|	catalysts			
parameters	free AuBP	free AuNR	PAH/DS/AuBP capsules	PAH/DS/AuNR capsules
length of ANP (nm)	20–25	25–30	20–25	25–30
diameter of capsules (μm)			3.5 ± 0.25	3.5 ± 0.25
weight of ANPs (g/mL)	6.67×10^{-4}	1.67×10^{-4}		
no. of ANPs/mL	1.16×10^{14}	5.72×10^{12}		
weight of capsules (g/mL)			2.5×10^{-3}	2×10^{-3}
no. of capsules/mL			3.6×10^{8}	2.9×10^{8}
weight of ANPs in capsules (g/mL)			2.5×10^{-3}	5×10^{-4}
no. of ANPs in the capsules/mL			4.4×10^{14}	1.7×10^{13}
rate constant (s^{-1})	1.04×10^{-3}	1.3×10^{-3}	9.7×10^{-4}	1.3×10^{-3}
conversion time (min)	65	45	85	60
catalyst (g)/g of PNP	0.26	0.03	0.21	0.52
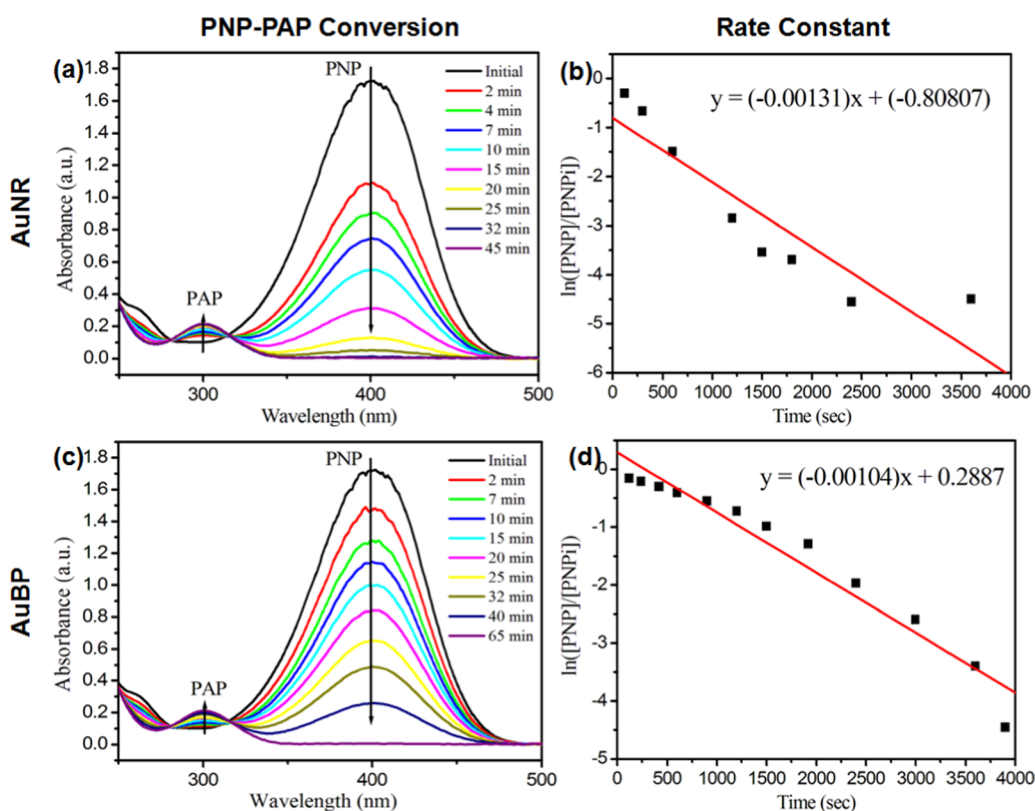
Figure 4. Kinetic trends of PNP–PAP reaction at different time intervals and the corresponding plots of $\ln([PNP]/[PNP_i])$ vs time for (a, b) free AuNRs and (c, d) free AuBPs as catalysts.

microcapsules, were prepared and used for catalytic conversion of PNP. The sample details are summarized in Table 1. The reaction was started by adding a specific amount of catalyst NPs (free NPs or microreactors) to the aqueous solution of PNP and NaBH$_4$. The conversion of PNP to PAP was monitored by observing the PNP characteristic peak at 400 nm using UV–vis spectroscopy. With increase in time, the absorption peak at 400 nm started to decrease, which indicated the reduction of PNP. At the same time, the appearance of a new peak at 300 nm confirmed the formation of PAP. As expected, control capsules without ANPs did not initiate the reaction.

2.2.1. Conversion by Free ANPs in Suspension. PNP conversion started as soon as a specific amount of free AuNRs (~1.67×10^{-4} g/mL) or free AuBPs (~6.67×10^{-4} g/mL) was added into the aqueous mixture of PNP and NaBH$_4$, as

shown in Figure 4. The time required to achieve 100% conversion was 45 and 65 min for AuNR and AuBP, respectively. Although the amount of catalyst NPs used for AuNRs was less, the reaction took place at a higher rate for AuNRs than for AuBPs. Previous reports showed that chemisorption of hydrogen molecules was more on low-coordinated gold atoms, i.e., NPs with more corner and edge sites.[38] AuBPs do have more edged sites, but the reaction was found to be slower compared to AuNRs. It is possible that the effective surface area available for reduction process was less for AuBPs. The rate constants were calculated corresponding to the negative slope of $\ln([PNP]/[PNP_i])$ vs time, where [PNP] denotes the concentration of PNP at different time points and [PNP$_i$] denotes the initial concentration of PNP at the start of the reaction (Figure 4). The calculated rate constants were 0.00131 s^{-1} for AuNRs and 0.00104 s^{-1} for

Figure 5. Kinetic trends of PNP−PAP reaction at different time intervals and the corresponding plots of $\ln([\text{PNP}]/[\text{PNP}_i])$ vs time for (a, b) PAH/DS/AuNR microcapsules and (c, d) PAH/DS/AuBP microcapsules as catalysts.

AuBPs. Approximately, 0.03 and 0.26 g of free AuNRs and AuBPs, respectively, were required as catalysts to convert per gram of PNP.

2.2.2. Conversion by Microreactor Capsules. To estimate the catalytic activity, catalyst in capsule form was added to the reactant solution while keeping other parameters constant. Notably, microreactors retained their catalytic activity and catalyzed the PNP-to-PAP conversion process. The conversion is a multistep process as follows: (a) movement of $NaBH_4$ and PNP from bulk to the capsule shell, (b) transport of $NaBH_4$ and PNP from shell to interior and to ANP surface, (c) hydride formation and conversion to PAP, and (d) desorption from the surface and backward movement to bulk. As the reactants and products had to move through porous shell, the time required to achieve 100% conversion was more for microreactor system compared to free ANPs. The amounts of microreactor capsules used were ∼2 × 10^{-3} g/mL for PAH/DS/AuNR capsules and ∼2.5 × 10^{-3} g/mL for PAH/DS/AuBP capsules. Figure 5 shows UV−vis spectra and the linear trends obtained during the catalysis reaction. The time required for total conversion was 60 and 85 min for microreactors with AuNRs and AuBPs, respectively. Interestingly, the rate of AuNR-catalyzed reaction was higher compared to the AuBP system, and the trend was also matching well with free NPs in suspension. The estimated rate constant values were 0.00125 s^{-1} for PAH/DS/AuNR capsules and 0.00097 s^{-1} for PAH/DS/AuBP capsules, which depicted their efficiency as microreactors. To investigate the reusability of the capsule system, microreactors were separated by centrifugation and dispersed in fresh reactant solution, and experiments were conducted for three continuous cycles. Similarly to the first cycle, 100% conversion was achieved for the second and third cycles also, however, with a slight increase

in conversion time. The time required for 100% conversion was 45, 58, and 70 min for the first, second, and third cycles, respectively. Approximately, 0.52 and 0.21 g of PAH/DS/AuNRs and PAH/DS/AuBP capsules, respectively, were required as catalysts to convert per gram of PNP. To investigate the role of aspect ratio of NRs, microreactors with NRs of varying aspect ratio ranging from 2 to 4.7 were synthesized and used for catalysis. The time required for complete conversion of PNP was 70, 77, and 72 min for NRs of aspect ratios 2.67, 3, and 4, respectively. Previous report showed that the rate of reaction was slightly higher for longer NRs (aspect ratio = 33 ± 0.5) compared to shorter NRs (aspect ratio = 2.8 ± 0.2).[24] However, we did not observe any difference in conversion time and rate constants. We believe that only larger difference in aspect ratio of the NRs might significantly influence the rate of the reaction.

For comparative study, the PAP conversion of different systems was estimated as a function of time (Figure 6). Even though larger amounts of free and capsule forms of AuBPs displayed an efficient catalytic activity, they were slower than AuNRs. Overall, AuNRs in free and capsule forms were better than AuBPs in free and capsule forms. Notably, rate constants were 1.31 times greater than those of previous reports for free AuNRs in suspension.[23] Furthermore, the amount of catalyst required to convert 1 g of PNP was much lower for our systems. Hence, these results proved that the reported systems have high potential for use as microreactors with better catalytic activity and reusability.

3. CONCLUSIONS

We demonstrate highly efficient and reusable microreactor hollow capsule system encapsulated with AuNRs and AuBPs for catalysis application. Microreactor capsules made of PAH
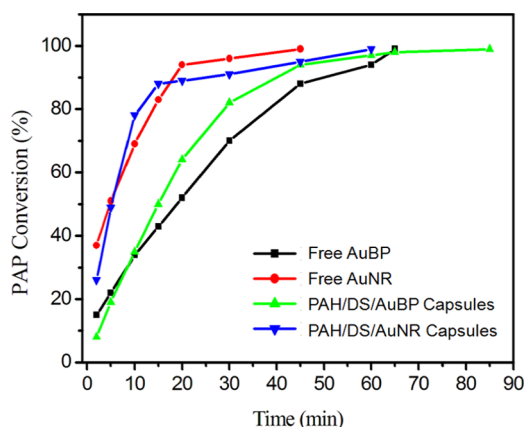
Figure 6. Conversion of PAP as a function of time for different catalyst systems.

and DS were prepared by modified template approach, wherein $CaCO_3$ microparticles containing preformed AuNRs or AuBPs were used as sacrificial template for LbL assembly to fabricate PAH/DS/AuNR or PAH/DS/AuBP capsules. Well-dispersed and stable ANPs of size 25−30 nm were observed in the interior of the microreactor capsule system. Microreactors showed excellent catalytic activity for reduction of PNP to PAP in the presence of $NaBH_4$ in aqueous phase. Reaction kinetics demonstrated that the reaction was of pseudo-first order. A 100% conversion was achieved for all of the catalyst systems, and the reaction rate was higher for AuNRs in capsule and free forms compared to AuBPs. The increase in aspect ratio of AuNRs from 2 to 4.7 did not significantly influence the conversion and rate constants. Microreactors retained catalytic activity even after three cycles and confirmed the reusability of the reported system. The methodology and microreactor system reported here can be useful for other shapes also and will be useful in various applications such as catalysis, drug delivery, and imaging.

4. MATERIALS AND METHODS

4.1. Chemicals. Gold(III) chloride trihydrate ($HAuCl_4$), PAH (M_w = 17 500 Da), DS (M_w > 500 000 Da), AA, EDTA and CTAB were purchased from Sigma-Aldrich. Other chemicals such as $NaBH_4$, sodium carbonate (Na_2CO_3), sodium citrate, calcium chloride ($CaCl_2$), silver nitrate ($AgNO_3$), and PNP were purchased from SRL India Pvt. Ltd. Poly(styrenesulfonate) (PSS, M_w = 70 000) was received from Alfa Aesar Pvt. Ltd. All chemicals were of analytical grade and used without further purification. All of the experiments were performed with freshly prepared stock solution. Milli-Q water with resistivity >18.2 MΩ cm at 25 °C from Millipore water purification system was used for all experiments.

4.2. Synthesis of AuNRs. The AuNRs with aspect ratio of 4 ± 0.3 were synthesized by seed-mediated approach according to a previously reported method.[35] The Au seed was prepared by adding 0.6 mL of ice-cold $NaBH_4$ into 10 mL of solution containing 0.1 M CTAB and 0.25 mM $HAuCl_4$ while continuously stirring at 25 °C. After addition, the solution turned yellowish brown, indicating the formation of seed crystals of ~4 nm with maximum absorption at 475 nm. After storing the seed crystals for 45 min, they were grown into NRs by mixing 12 μL of seed into a 10 mL solution of 0.1 M CTAB and 0.5 mM $HAuCl_4$ with 200 μL of $AgNO_3$ and 70 μL of AA. Color change to violet was observed within 30 min, and the

absorption spectrum was acquired to confirm the formation of NRs. The NRs were then washed thrice with water for further use. AuNRs with aspect ratio ranging from 2 to 4.7 were prepared by varying the $AgNO_3$ concentration (100, 150, and 300 μL) during the growth process.

4.3. Synthesis of AuBPs. A seeding growth process with $AgNO_3$ was applied for the synthesis of AuBPs as reported earlier.[36] The Au seed here was prepared by adding 0.6 mL of ice-cold solution of $NaBH_4$ into a mixture of 0.2 mL of 2.5 mM trisodium citrate and 19.8 mL of 0.25 mM $HAuCl_4$. The citrate ions served as capping agent at this step, which allowed growth of particles in [110] and [111] facets.[36] The solution turned orange red, confirming the formation of seed. For the preparation of growth solution, two solutions A and B containing 9 mL of a solution of 0.25 mM $HAuCl_4$ and 0.1 M CTAB were prepared for the stepwise growth of AuBPs. $AgNO_3$ (100 μL) was added only to B, while 50 μL of AA was added to both A and B. Thereafter, 1 mL of seed solution was added to A for 10 s under stirring and 1 mL of this solution was immediately transferred to B. Violet color was observed after incubation of solution B at 30 °C for 12 h, which was then investigated using a UV−vis spectrophotometer. Finally, it was washed thrice to obtain AuBPs for further use.

4.4. Synthesis of Modified $CaCO_3$ Template for LbL Assembly. The modified sacrificial template was synthesized by adding preformed AuNRs or AuBPs during the formation of $CaCO_3$ template by colloidal crystallization method.[29] In brief, equimolar solutions of 0.3 M Na_2CO_3 and $CaCl_2$ were prepared in water. Prior to synthesis process, PSS solution (1 mg/mL) and suspension of preformed AuNRs/AuBPs were added to Na_2CO_3 solution. Finally, $CaCl_2$ solution was added in a dropwise manner to form colloidal $CaCO_3$−AuNR or $CaCO_3$−AuBP templates. PSS was added to impart stability to the synthesized templates. This template was finally washed thrice with water and dried for further use.

4.5. Fabrication of PAH/DS Microreactor Capsules Incorporated with AuNR or AuBP. The microreactor PAH/DS capsules containing AuNRs (PAH/DS/AuNRs) or AuBPs (PAH/DS/AuBPs) in the inner hollow structure were fabricated by the LbL approach. The modified template (either $CaCO_3$−AuNRs or $CaCO_3$−AuBPs) was dispersed in 2 mL of 1 mg/mL PAH solution for 15 min. The polymer-coated particles were separated by centrifugation at 5000 rpm (Hermle Labortechnik, Germany) and washed thrice with Milli-Q water to remove loosely bound PAH molecules. The particles coated with PAH layer were dispersed again in DS for 15 min, and washing was done three times with Milli-Q water. One layer of PAH and one layer of DS was termed as one bilayer. After deposition of two bilayers of PAH and DS, the core was dissolved using 0.2 M EDTA solution to obtain hollow capsules containing AuNRs/AuBPs in their inner structure.

4.6. Conversion of PNP to PAP Using Microreactor Capsules. Capsules with encapsulated NRs or BPs were investigated for their catalytic activity for the reduction of PNP to PAP, as shown in Scheme 1. Capsules prepared in a single batch were used for catalytic experiments to get consistent results. To estimate the number of capsules and amount of NPs in the capsules, a capsule suspension of 1 mL was first dried at 80 °C for 2 h (until there is no weight difference) and the final weight (combined weight of capsule and ANPs) was measured. The mass of ANPs present in 1 mL of capsule suspension was estimated by burning the dried capsule mass in

a tubular furnace at 400 °C for 1.5 h. Average sizes of NPs and capsules were estimated by measuring individual sizes of at least 100 NPs or capsules from TEM images. By using the density and average size of gold NPs and capsules, the total number of capsules and particles per unit volume of the suspension was estimated.

Prior to catalytic conversion, 1 mL of 1 mM PNP was mixed with 1 mL of 0.1 mol/L $NaBH_4$. Specific amounts of aqueous sample containing microreactor capsules (30 μL of PAH/DS/AuNR microcapsule stock having 2.9×10^8 capsules or 55 μL of PAH/DS/AuBP microcapsule stock having 3.6×10^8 capsules) were added to the mixture to start the reaction as specified in Table 1. The reaction kinetics was studied by measuring the absorbance of PNP at 400 nm using UV−vis spectroscopy at different time intervals. After the completion of the reaction, the PNP solution turned from yellow to colorless, indicating the formation of reduced product PAP. The same experiments were repeated with free AuBPs or AuNRs as catalysts for investigation of the effectiveness of microreactor capsules. The conversion time and rate constants were estimated using the initial PNP concentration and concentration at different time points. The rate constants were calculated from the slope of $\ln([PNP]/[PNP_i])$ vs time curve, where [PNP] is the concentration of PNP at a particular time interval and $[PNP_i]$ is the initial concentration. The kinetic data satisfactorily fitted the pseudo-first-order kinetic reaction as shown below.
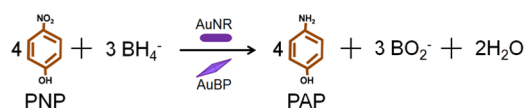
4.7. UV−Visible Spectroscopy. UV−vis absorption spectra were recorded on a NanoDrop 2000c Spectrophotometer (NanoDrop Technologies) using Milli-Q water as blank. UV−vis spectra were acquired by directly keeping 4 μL of free ANPs or microreactor capsules suspension on the pedal of the UV−vis spectrophotometer. For catalysis experiments, the PNP concentration was estimated at predetermined time points to calculate the reaction rate constants and % conversion.

4.8. Transmission Electron Microscopy. The sample preparation for TEM analysis was done by placing 4 μL of sample on carbon-coated copper grid and dried overnight to remove the moisture completely. TEM images of free ANPs and microreactor capsules were acquired using a high-resolution transmission electron microscope (JEOL TEM 2100 Plus, Japan) at an accelerating voltage of 200 kV.

■ AUTHOR INFORMATION

Corresponding Author
*E-mail: rsanandhakumar@gmail.com, anandhakumar.s@res.srmuniv.ac.in. Tel: +91-4427417902 (Off), Mob: +918838104529.

ORCID ⊙
Anandhakumar Sundaramurthy: 0000-0001-6870-7318

Notes
The authors declare no competing financial interest.

■ REFERENCES

(1) Guzmán, E.; Mateos-Maroto, A.; Ruano, M.; Ortega, F.; Rubio, R. G. Layer-by-Layer polyelectrolyte assemblies for encapsulation and release of active compounds. *Adv. Colloid Interface Sci.* **2017**, *249*, 290−307.

(2) Postupalenko, V.; Einfalt, T.; Lomora, M.; Dinu, I. A.; Palivan, C. G. Bionanoreactors: From Confined Reaction Spaces to Artificial Organelles. In *Organic Nanoreactors*; Elsevier, 2016; pp 341−371.

(3) Balasubramanian, V.; Herranz-Blanco, B.; Almeida, P. V.; Hirvonen, J.; Santos, H. A. Multifaceted polymersome platforms: Spanning from self-assembly to drug delivery and protocells. *Prog. Polym. Sci.* **2016**, *60*, 51−85.

(4) Caruso, F. *Modern Techniques for Nano-and Microreactors/-Reactions*; Springer, 2010; p 229.

(5) Mura, S.; Nicolas, J.; Couvreur, P. Stimuli-responsive nanocarriers for drug delivery. *Nat. Mater.* **2013**, *12*, 991−1003.

(6) Tanner, P.; Balasubramanian, V.; Palivan, C. G. Aiding nature's organelles: artificial peroxisomes play their role. *Nano Lett.* **2013**, *13*, 2875−2883.

(7) Hammer, D. A.; Kamat, N. P. Towards an artificial cell. *FEBS Lett.* **2012**, *586*, 2882−2890.

(8) Anraku, Y.; Kishimura, A.; Kamiya, M.; Tanaka, S.; Nomoto, T.; Toh, K.; Matsumoto, Y.; Fukushima, S.; Sueyoshi, D.; Kano, M. R.; et al. Systemically Injectable Enzyme-Loaded Polyion Complex Vesicles as In Vivo Nanoreactors Functioning in Tumors. *Angew. Chem., Int. Ed.* **2016**, *55*, 560−565.

(9) Anandhakumar, S.; Debapriya, M.; Nagaraja, V.; Raichur, A. M. Polyelectrolyte microcapsules for sustained delivery of water-soluble drugs. *Mater. Sci. Eng., C* **2011**, *31*, 342−349.

(10) Sun, H.; Cui, J.; Ju, Y.; Chen, X.; Wong, E. H.; Tran, J.; Qiao, G. G.; Caruso, F. Tuning the properties of polymer capsules for cellular interactions. *Bioconjugate Chem.* **2017**, *28*, 1859−1866.

(11) Chandrawati, R. Layer-by-Layer Engineered Polymer Capsules for Therapeutic Delivery. In *Biomaterials for Tissue Engineering*; Springer, 2018; Vol. *1758*, pp 73−84.

(12) Anandhakumar, S.; Nagaraja, V.; Raichur, A. M. Reversible polyelectrolyte capsules as carriers for protein delivery. *Colloids Surf., B* **2010**, *78*, 266−274.

(13) Paramasivam, G.; Vergaelen, M.; Ganesh, M.-R.; Hoogenboom, R.; Sundaramurthy, A. Hydrogen bonded capsules by layer-by-layer assembly of tannic acid and poly (2-n-propyl-2-oxazoline) for encapsulation and release of macromolecules. *J. Mater. Chem. B* **2017**, *5*, 8967−8974.

(14) Larrañaga, A.; Lomora, M.; Sarasua, J.-R.; Palivan, C. G.; Pandit, A. Polymer capsules as micro-/nanoreactors for therapeutic applications: Current strategies to control membrane permeability. *Prog. Mater. Sci.* **2017**, *90*, 325−357.

(15) Ermakov, A. V.; Inozemtseva, O. A.; Gorin, D. A.; Sukhorukov, G. B.; Belyakov, S.; Antipina, M. N. Influence of Heat Treatment on Loading of Polymeric Multilayer Microcapsules with Rhodamine B. *Macromol. Rapid Commun.* **2018**, *428*, No. e1800200.

(16) Anandhakumar, S.; Vijayalakshmi, S.; Jagadeesh, G.; Raichur, A. M. Silver nanoparticle synthesis: novel route for laser triggering of polyelectrolyte capsules. *ACS Appl. Mater. Interfaces* **2011**, *3*, 3419−3424.

(17) Anandhakumar, S.; Raichur, A. M. Polyelectrolyte/silver nanocomposite multilayer films as multifunctional thin film platforms for remote activated protein and drug delivery. *Acta Biomater.* **2013**, *9*, 8864−8874.

(18) Anandhakumar, S.; Mahalakshmi, V.; Raichur, A. M. Silver nanoparticles modified nanocapsules for ultrasonically activated drug delivery. *Mater. Sci. Eng., C* **2012**, *32*, 2349−2355.

(19) Stavarache, C. E.; Paniwnyk, L. Controlled rupture of magnetic LbL polyelectrolyte capsules and subsequent release of contents employing high intensity focused ultrasound. *J. Drug Delivery Sci. Technol.* **2018**, *45*, 60−69.

(20) De Koker, S.; De Cock, L. J.; Rivera-Gil, P.; Parak, W. J.; Velty, R. A.; Vervaet, C.; Remon, J. P.; Grooten, J.; De Geest, B. G. Polymeric multilayer capsules delivering biotherapeutics. *Adv. Drug Delivery Rev.* **2011**, *63*, 748−761.

(21) Liu, Y.; Xu, L.; Liu, X.; Cao, M. Hybrids of gold nanoparticles with core-shell hyperbranched polymers: Synthesis, characterization, and their high catalytic activity for reduction of 4-nitrophenol. *Catalysts* **2016**, *6*, 3.

(22) Li, G.; Jin, R. Catalysis by gold nanoparticles: carbon-carbon coupling reactions. *Nanotechnol. Rev.* **2013**, *2*, 529−545.

(23) de Oliveira, F. M.; Nascimento, L. R. B. dA.; Calado, C. M. S.; Meneghetti, M. R.; da Silva, M. G. A. Aqueous-phase catalytic chemical reduction of p-nitrophenol employing soluble gold nanoparticles with different shapes. *Catalysts* **2016**, *6*, No. 215.

(24) Kundu, S.; Lau, S.; Liang, H. Shape-controlled catalysis by cetyltrimethylammonium bromide terminated gold nanospheres, nanorods, and nanoprisms. *J. Phys. Chem. C* **2009**, *113*, 5150−5156.

(25) Soetan, N.; Zarick, H. F.; Banks, C.; Webb, J. A.; Libson, G.; Coppola, A.; Bardhan, R. Morphology-directed catalysis with branched gold nanoantennas. *J. Phys. Chem. C* **2016**, *120*, 10320−10327.

(26) Somorjai, G. New model catalysts (platinum nanoparticles) and new techniques (SFG and STM) for studies of reaction intermediates and surface restructuring at high pressures during catalytic reactions. *Appl. Surf. Sci.* **1997**, *121−122*, 1−19.

(27) Wang, J.; Zhu, C.; Han, J.; Han, N.; Xi, J.; Fan, L.; Guo, R. Controllable Synthesis of Gold Nanorod/Conducting Polymer Core/Shell Hybrids Toward in Vitro and in Vivo near-Infrared Photothermal Therapy. *ACS Appl. Mater. Interfaces* **2018**, *10*, 12323−12330.

(28) Chen, X.; Zhang, Q.; Li, J.; Yang, M.; Zhao, N.; Xu, F.-J. Rattle-Structured Rough Nanocapsules with In-Situ Formed Gold Nanorod Cores for Complementary Gene/Chemo/Photothermal Therapy. *ACS Nano* **2018**, *12*, 5646−5656.

(29) Chen, H.; Di, Y.; Chen, D.; Madrid, K.; Zhang, M.; Tian, C.; Tang, L.; Gu, Y. Combined chemo-and photo-thermal therapy delivered by multifunctional theranostic gold nanorod-loaded microcapsules. *Nanoscale* **2015**, *7*, 8884−8897.

(30) Skirtach, A. G.; De Geest, B. G.; Mamedov, A.; Antipov, A. A.; Kotov, N. A.; Sukhorukov, G. B. Ultrasound stimulated release and catalysis using polyelectrolyte multilayer capsules. *J. Mater. Chem.* **2007**, *17*, 1050−1054.

(31) Hussain, S. Z.; Zyuzin, M. V.; Hussain, I.; Parak, W. J.; Carregal-Romero, S. Catalysis by multifunctional polyelectrolyte capsules. *RSC Adv.* **2016**, *6*, 81569−81577.

(32) Anandhakumar, S.; Sasidharan, M.; Tsao, C.-W.; Raichur, A. M. Tailor-made hollow silver nanoparticle cages assembled with silver nanoparticles: An efficient catalyst for epoxidation. *ACS Appl. Mater. Interfaces* **2014**, *6*, 3275−3281.

(33) Li, X.; Cai, T.; Kang, E.-T. Hairy Hybrid Nanorattles of Platinum Nanoclusters with Dual-Responsive Polymer Shells for Confined Nanocatalysis. *Macromolecules* **2016**, *49*, 5649−5659.

(34) He, X.; Liu, Z.; Fan, F.; Qiang, S.; Cheng, L.; Yang, W. Poly (ionic liquids) hollow nanospheres with PDMAEMA as joint support of highly dispersed gold nanoparticles for thermally adjustable catalysis. *J. Nanopart. Res.* **2015**, *17*, No. 74.

(35) Nikoobakht, B.; El-Sayed, M. A. Preparation and growth mechanism of gold nanorods (NRs) using seed-mediated growth method. *Chem. Mater.* **2003**, *15*, 1957−1962.

(36) Wu, H.-L.; Chen, C.-H.; Huang, M. H. Seed-mediated synthesis of branched gold nanocrystals derived from the side growth of pentagonal bipyramids and the formation of gold nanostars. *Chem. Mater.* **2009**, *21*, 110−114.

(37) Goepel, M.; Al-Naji, M.; With, P.; Wagner, G.; Oeckler, O.; Enke, D.; Gläser, R. Hydrogenation of p-Nitrophenol to p-Aminophenol as a Test Reaction for the Catalytic Activity of Supported Pt Catalysts. *Chem. Eng. Technol.* **2014**, *37*, 551−554.

(38) Stobiński, L.; Zommer, L.; Duś, R. Molecular hydrogen interactions with discontinuous and continuous thin gold films. *Appl. Surf. Sci.* **1999**, *141*, 319−325.